Surface functionalization of magnetic mesoporous silica nanoparticles for controlled drug release. J Mater Chem

ARTICLE *in* JOURNAL OF MATERIALS CHEMISTRY · NOVEMBER 2010

Impact Factor: 7.44 · DOI: 10.1039/C0JM01237H

5 AUTHORS, INCLUDING:

Jia Guo
Fudan University
87 PUBLICATIONS **2,433** CITATIONS
SEE PROFILE

Wuli Yang
Fudan University
154 PUBLICATIONS **4,558** CITATIONS
SEE PROFILE

Surface functionalization of magnetic mesoporous silica nanoparticles for controlled drug release

Baisong Chang,[a] Jia Guo,[a] Congying Liu,[a] Ji Qian[b] and Wuli Yang*[a]

Received 28th April 2010, Accepted 28th July 2010
DOI: 10.1039/c0jm01237h

The modified sol–gel approach to the synthesis of well-structured magnetic mesoporous silica nanoparticles (M-MSNs) was described, which comprised magnetic nanoparticles resided within the mesoporous nanoparticles. A diversity of surface modification was subjected to systematic investigation using organic silanes, eventually resulting in the decoration with the carboxyl (–COOH), methyl phosphonate ($–PO_3^-$), amino ($–NH_2$) and phenyl (–Ph) groups on the surface of M-MSNs. The careful characterizations demonstrated that the modified M-MSNs displayed the specifically charged surfaces and differently porous characters, yet without showing any influence on the shape and size. To exploit their potential in cancer treatment, we extensively studied the drug loading capacity and sustained release behaviour of the modified M-MSNs for representative drugs. The hydrophilically modified M-MSNs with –COOH and $–PO_3^-$ were beneficial for loading the water-soluble doxorubicin hydrochloride (DOX) through electrostatic attraction. The results demonstrated that M-MSNs-PO_3^- achieved a higher loading content and M-MSNs-COOH presented a distinct pH-responsible release behavior. On the other hand, M-MSNs-Ph displayed a controlled release rate in a short term *via* the weakened hydrogen bonding interaction. The cytotoxicity of modified M-MSNs to normal cells and macrophage uptake indicated that the modified M-MSNs were suitable as drug carriers. These mesoporous nanoparticles were non-toxicity to HeLa cells, while the drug-loaded nanoparticles apparently led to the unambiguous cytotoxicity as a result of the sustained release of drugs. These results have an important implication that the modified M-MSNs are promising as platforms for storing the hydrophilic or hydrophobic anticancer drugs for tumour therapy.

Introduction

Nano-scaled drug carriers have evoked much interest due to their enhanced permeability and retention (EPR) effect,[1,2] which facilitates drug delivery in cancerous tissues. To date, extensive studies have witnessed rapid advances in the elaborate synthesis of versatile drug carriers as platforms, such as polymeric micelles,[3] dendrimers[4] and liposomes.[5] Their potential applications have been well demonstrated by the excellent payload capacity for specific drugs in treating the cancerous tissues. However, since a variety of drugs has their respective solubility in physiological medium,[6,7] it is impossible that the carriers allow their inner chemical environments to have the strong affinity to polar and non-polar molecules spontaneously. Thus, once drug carriers are needed to load the various anticancer drugs, it is still a significant challenge up to now. As a result, our objective of the current work is to exploit the flexible ability of drug carriers to bear the hydrophobic or hydrophilic drugs and to systematically investigate their *in vitro* release behaviours.

In contrast with the prior known organic drug carriers, mesoporous silica nanoparticles (MSNs) exhibit distinctive advantages including large surface area, high pore volume, and prominent biocompatibility.[8,9] These superior properties endow MSNs with exceptional capacity for drug storage.[8,10–12] More intriguingly, the superficial silanol groups resided on MSNs can be utilized to functionalize by organic silanes,[13–15] as expected to deliberately control the drug–surface interaction.[16] To the best of our knowledge, there are two main methods well reported until now, *i.e.* co-condensation and post-grafting modification.[17] In comparison with the co-condensation, the post-grafting strategy not only retains the well-ordered mesostructure of the original silica phase, but also provides a large amount of function groups for conveniently entrapping drugs within mesopores. For example, the modification with -NH_2 groups on MSNs could facilitate the payload and sustained release of ibuprofen.[18] As a result, it is most likely to accomplish the load of various drugs by tuning the surface properties of MSNs.

Magnetic nanoparticles, due to their superparamagnetic behaviour, lead to a wide range of disciplines, including magnetic resonance imaging (MRI),[19,20] catalysis,[21] protein separations[22] and drug target delivery.[23] It was noticed that some interesting work that described the facile approach to synthesize the magnetic mesoporous silica nanoparticles (M-MSNs) in order to achieve a site-selective drug delivery.[24] However, tremendous efforts merely focused on the construction of well-defined structure,[25] irrespective of developing the drug loading and release systematically.

In this work, we prepared a series of M-MSNs with various organic groups on the surface, and performed a systematic

[a]*Key Laboratory of Molecular Engineering of Polymers (Ministry of Education) and Department of Macromolecular Science, Fudan University, Shanghai, 200433, China. E-mail: wlyang@fudan.edu.cn*
[b]*State Key Laboratory of Genetic Engineering and Key Laboratory of Contemporary Anthropology (Ministry of Education), School of Life Sciences and Institutes of Biomedical Sciences, Fudan University, Shanghai, China*

investigation on loading the anticancer drugs within the modified M-MSNs. In place of ibuprofen that is widely tested as a common anti-inflammatory agent,[26] we herein employed other two model drugs, *i.e.* doxorubicin hydrochloride (DOX) and paclitaxel (PTX), both of which are currently in clinical use as anticancer drugs and show the typical characters of charges and hydrophobicity, respectively. In our studies, the detailed results indicated that the M-MSNs were readily functionalized with organic silanes and thus presented the flexible ability to store and release hydrophilic and hydrophobic drugs. The cytotoxicity to normal cells and macrophage uptake for the modified M-MSNs were evaluated. The *in vitro* cellular cytotoxicity of the drug-loaded nanoparticles towards HeLa cells was also unambiguously demonstrated.

Experimental

1. Materials and methods

1.1. Materials. Hydrophobic Fe_3O_4 nanoparticles with a diameter of about 15 nm were synthesized according to a previous report.[27] DOX in the form of the hydrochloride salt was obtained from Bejing Huafeng United Technology Company. PTX was purchased from Jiangsu Yew Pharmaceutical Company. Phenyltriethoxysilane (PTS) was purchased from Zhejiang Chemical Technology Company. Trihydroxysilylpropyl methylphosphonate (THMP) was purchased from Sigma-Aldrich. Tetraethyoxysilane (TEOS), cetyltrimethylammonium bromide (CTAB), 3-aminopropyltriethoxysilane (APS), succine anhydride and ammonium nitrate (NH_4NO_3) were obtained from Shanghai Chemical Reagents Company. The other chemicals used were of reagent grade and were used without further purification.

1.2. Synthesis of M-MSNs. M-MSNs were prepared by the sol–gel method.[24,28] Briefly, 7.5 mg of Fe_3O_4 nanoparticles dispersed in 1 mL of chloroform was mixed with 10 mL of aqueous solution containing 0.1 g of CTAB under vigorous stirring. The chloroform was evaporated at 65 °C to give the CTAB-Fe_3O_4 dispersion. Then, 90 mL of distilled water was added. The mixture was stirred quickly for 2 h at 40 °C. Finally, 3 mL of aqueous ammonia solution (25 wt%), 0.5 mL of TEOS and 5 mL of ethyl acetate were successively added to the above mixture with rapid stirring for 1 min, and then kept at 80 rpm for another 6 h at 40 °C. The synthesized product was centrifuged, washed with distilled water and ethanol for several times.

In order to load drug molecules into M-MSNs, further purification through ion exchange was conducted[29] for removal of the structure-directing CTAB. The as-synthesized product was dispersed in the ethanol solution of NH_4NO_3 (60 mL, 10 mg mL^{-1}). The mixture was refluxed for 6 h, then collected by centrifugation and washed with ethanol repeatedly. Finally, the obtained product dried under vacuum to give the brownish powder.

1.3. Functionalization of M-MSNs. M-MSNs were functionalized with $–NH_2$, $–PO_3^-$ and –Ph using the post-grafting method.[16] Typically, 0.1 g of M-MSNs was dispersed in 50 mL of ethanol. Following the addition of organic silanes (0.6 mmol), the mixture was stirred moderately at 80 °C for 6 h. The precipitate was collected by centrifugation, washed with ethanol and dried under vacuum. The obtained modified M-MSNs, which were subjected to the post-grafting of APS, THMP and PTS, were denoted as the M-MSNs-NH_2, M-MSNs-PO_3^- and M-MSNs-Ph, respectively.

The –COOH functionalization of M-MSNs was carried out in *N*,*N*′-dimethylformamide (DMF). 0.1 g of M-MSNs-NH_2 was added in the DMF solution of succinic anhydride (50 mL, 2 wt%). The mixture was stirred for 24 h at room temperature. After that, the product was collected by centrifugation, washed with ethanol and dried under vacuum. The synthesized sample was denoted as M-MSNs-COOH.

1.4. Drug loading experiments

(1) DOX. DOX was dissolved in distilled water with a concentration of 0.5 mg mL^{-1}. 5 mg of M-MSNs-COOH was ultrasonically dispersed in 5 mL of the DOX solution. The mixture was stirred at room temperature for 24 h. Then the dispersion was centrifuged to collect the DOX-loaded nanoparticles and kept the supernatant for calculating the drug loading content. In order to remove the DOX on the exterior surface of M-MSNs-COOH, the drug-loaded nanoparticles were washed with distilled water for twice and collected by centrifugation. The supernatant in the washing process was combined with the previous supernatant solution. The mass of DOX loaded into M-MSNs-COOH was calculated by subtracting the mass of DOX in the supernatant from the total mass of drug in the initial solution. The amount of DOX adsorbed was analyzed with UV-vis at the wavelength of 480 nm. The experiments for loading DOX into M-MSNs-PO_3^- and M-MSNs followed the same procedure as above described. The drug loading content and entrapment efficiency were calculated using the eqn (1) and (2), respectively:

$$\text{Loading content (\%)} = \frac{\text{Mass of drug in mesoporous silica}}{\text{Mass of drug loaded mesoporous silica}} \quad (1)$$

$$\text{Entrapment efficiency (\%)} = \frac{\text{Mass of drug in mesoporous silica}}{\text{Initial mass of drug}} \quad (2)$$

(2) PTX. For encapsulating PTX into M-MSNs-Ph, 20 mg of M-MSNs-Ph was dispersed in dichloromethane solution of PTX (2 mL, 1 mg mL^{-1}). The solution was stirred for 2 d in a sealed vial. Then the PTX-loaded nanoparticles were collected by centrifugation, washed with distilled water for twice, and dried under vacuum at 45 °C overnight. To measure the loading content of PTX into M-MSNs-Ph, 5 mg of PTX-loaded nanoparticles were suspended in methanol. After 2 h, the nanoparticles were isolated by centrifugation and the supernatant was diluted for analysis using UV-vis at 227 nm. The same process of encapsulation of PTX within M-MSNs was implemented as above mentioned. The drug loading content and entrapment efficiency were also calculated using the eqn (1) and (2).

1.5. Drug release *in vitro*. To study the release behaviour, DOX-loaded nanoparticles were dispersed in 2 mL of PBS, and the dispersion was transferred into dialysis bag (molecular weight cut off 5000). The dialysis bag was then kept in 200 mL of PBS and gently shaken at 37 °C. At timed intervals, 1 mL of solution was withdrawn from the solution periodically and the amount of released drug was analyzed by UV-vis. For keeping constant volume, 1 mL of fresh medium was added after each sampling. All drugs release results were averaged with three measurements.

In PTX release experiments, the PTX-loaded nanoparticles were dispersed in 2 mL of PBS and the solution was placed in dialysis tubing (molecular weight cut off 5000). The dialysis tubing was immersed in 15 mL of PBS at 37 °C. The medium was replaced with fresh medium at various times. The amount of released PTX was determined using the UV-vis and all the release results were averaged with three measurements.

1.6. *In vitro* cell assays. The cytotoxicity assay was performed by using a cell-counting kit assay.[25] The HEK 293 (Human Embryonic Kidney) cells and HeLa cells were seeded into 96-well plates at 5000 cells per well and incubated for 24 h in a humidified atmosphere of 5% CO_2 at 37 °C. The HeLa cells were then washed with PBS and the medium was replaced with a fresh medium containing pure nanoparticles, free drugs, or the drug-loaded nanoparticles with the indicated concentrations. After 48 h, the cells were washed with PBS and incubated in DMEM with 10% WST-8 solution for 2 h. The absorbance of each well was measured at the wavelength of 450 nm with a plate reader. The results were expressed as mean values of three measurements. The same process of cytotoxicity analysis of pure nanoparticles to HEK 293 cells was implemented as above mentioned.

Human THP-1 monocyte cells were grown in RPMI 1640 medium supplemented with 10% heat-inactivated fetal bovine serum, 100 μg mL^{-1} penicillin and 100μg mL^{-1} streptomycin in 37 °C, 5% CO_2. To induce the monocyte to macrophage differentiation, THP-1 cells were cultured in 100 ng mL^{-1} phorbol-12-myristate-13-acetate for 48 h. Cells were washed with fresh media and treated with DOX-loaded M-MSNs-COOH with 50 μg mL^{-1} for 0.25, 0.5, 1, 2 and 4 h. The cells were washed once and the amount of uptake was quantified by fluorescence analysis.

2. Characterization

UV-vis spectra were obtained using a Perkin-Elmer Lambda 35 spectrophotometer. Nanoparticles were visualized using a JEOL 1230 transmission electron microscope (TEM). The size distribution of the nanoparticles was measured by dynamic light scattering (DLS) using an autosizer 4700 (Malvern). Zeta-potential was measured by Zetasizer Nano-ZS (Malvern). A vibrating-sample magnetometer (VSM) (EG & G Princeton Applied Research vibrating sample magnetometer, model 155) was used at 300 K to measure the magnetic moment. Thermogravimetric analysis (TGA) was carried out on a Pyrisis 1 TGA thermal analyzer from 100 to 700 °C (10 °C min^{-1}) in a flow of air. Nitrogen adsorption-desorption isotherms were obtained on a Micromeritics Tristar 3000 pore analyzer at 77 K under continuous adsorption conditions. Powder X-ray diffraction (PXRD) patterns were recorded on a Bruker D4 X-ray diffractometer with Ni-filtered Cu KR radiation (40 kV, 40 mA).

Result and discussion

1. Preparation of the functionalized M-MSNs

M-MSNs were prepared by the base-catalyzed sol–gel method in aqueous solution using the CTAB-coated Fe_3O_4 nanoparticles as seeds.[24] The TEM images displayed in Fig. 1A showed that the obtained M-MSNs had the uniform spherical shape with the

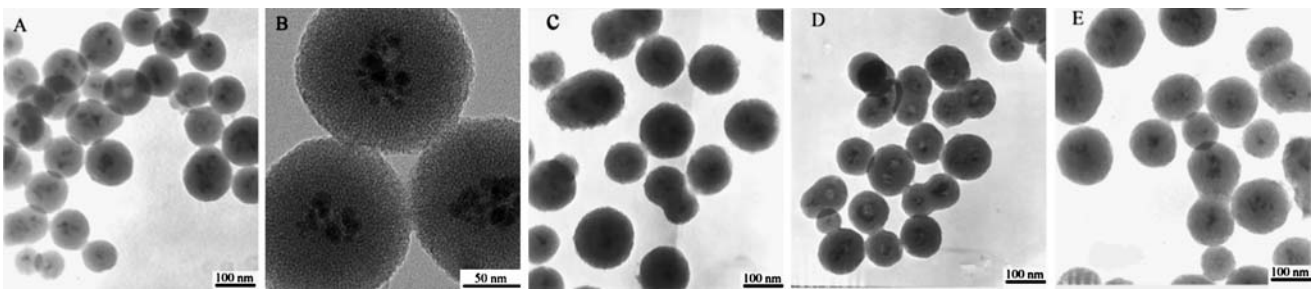

Fig. 1 TEM images of (A) M-MSNs, (B) M-MSNs at high magnification, (C) M-MSNs-Ph, (D) M-MSNs-PO_3^-, and (E) M-MSNs-COOH.

Table 1 DLS, N_2 sorption and TGA of samples described in the text

	DLS		N_2 sorption data			
Sample	Diameter/nm	PDI[a]	Surface area/m^2 g^{-1}	Pore volume/cm^3 g^{-1}	Pore diameter[b]/nm	Weight loss[c] (wt %)
M-MSNs	210	0.05	907	1.42	3.1	5.7
M-MSNs-NH_2	212	0.09	437	0.80	2.8	17.8
M-MSNs-COOH	218	0.08	299	0.54	2.6	20.6
M-MSNs-PO_3^-	219	0.06	417	1.03	2.9	16.3
M-MSNs-Ph	213	0.07	870	1.15	2.6	11.8

[a] PDI was the polydispersity index. [b] Pore diameter was calculated with the BJH method from the desorption branch. [c] The weight loss below 700 °C.

mean diameter of 130 ± 20 nm. A closer look at the fine structure (Fig. 1B) exhibited the multiple dark spots, *i.e.* Fe_3O_4 nanoparticles, were embedded within the center of M-MSNs matrix. Fig. 1C, 1D and 1E demonstrated that the modified M-MSNs preserved the typical composite structures and similar sizes, without showing any perturbance in the post-modification of M-MSNs.[17] In addition, the hydrodynamic diameter and size distribution were measured with DLS. Table 1 displayed that all of the samples had hydrodynamic diameters around 210 nm, larger than those observed in the TEM images because of the hydrate layer in an aqueous environment. The narrow size distributions for all the samples were verified by the small values of PDI (less than 0.10), indicative of exceptional water-dispersibility.

PXRD was conducted to determine the crystalline species of mesoporous structures. The PXRD pattern (Fig. 2A) showed apparent diffraction peaks due to (100), (110) and (200) planes, which agreed well with the highly ordered 2D hexagonal mesoporous structure.[11] The N_2 sorption profiles in Fig. 2B displayed type IV isotherms for all samples, implying the characteristic of mesopores. As listed in Table 1, the surface area, pore volume and pore diameter of M-MSNs were 907 $m^2\ g^{-1}$, 1.42 $cm^3\ g^{-1}$ and 3.1 nm, respectively. After post-grafting modification, these parameters of mesoporosity were correspondingly decreased. Especially, the synthesized M-MSNs-COOH showed the surface area and pore volume as small as 299 $m^2\ g^{-1}$ and 0.54 $cm^3\ g^{-1}$, respectively. This reducing tendency should be significantly attributed to the covalent fixation of organic groups on the M-MSNs.[30] When combined with the analysis of weight loss (Table 1), we further ensured that the variation in porosity was dependent on the grafting contents of organic groups on the modified M-MSNs. The magnetization were measured by VSM to give the field-dependent magnetic curves in Fig. 2D. It was evidently pointed out that no remanence at low applied magnetic field was detected at room temperature, suggesting that all the samples possessed the superparamagnetic behaviour.

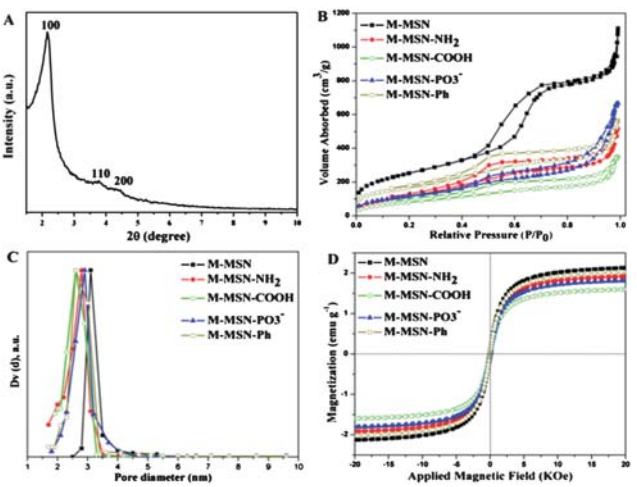

Fig. 2 (A) PXRD pattern of M-MSNs, (B) nitrogen adsorption-desorption isotherms, (C) pore diameters distribution and (D) field-dependent magnetization (300 K) of M-MSNs, M-MSNs-NH_2, M-MSNs-COOH, M-MSNs-PO_3^- and M-MSNs-Ph.

Table 2 Zeta-potential of samples at different pH values

	Zeta potential/mV		
Sample	pH = 4.2	pH = 7.4	pH = 9.3
M-MSNs	−10.2	−16.2	−32.8
M-MSNs-NH_2	42.1	21.7	−11.1
M-MSNs-COOH	20.3	−34.5	−52.1
M−MSNs−PO_3^-	−44.8	−48.3	−55.6
M-MSNs-Ph	−9.5	−13.8	−30.1

To characterize the surface charges of the samples, the zeta-potential measurement was performed. Table 2 showed the corresponding zeta potentials as a function of pH. In the case of M-MSNs, the zeta potentials decreased from −10.2 mV to −32.8 mV when the pH values increased from 4.2 to 9.3. As we know, the isoelectric point of silanol appears at pH = 1.5,[31] so that deprotonation of silanol groups induced the negative charges at high pH values. Oppositely, M-MSNs-NH_2 exhibited positive charges at pH = 7.4 and 4.2, and negative charge at pH = 9.3. This change suggested that -NH_2 groups were protonated in the acidic and neutral medium,[31] whereas their deprotonation in the alkaline medium allowed the residual silanol groups to afford the negative charge.[32] For M-MSNs-COOH, the negative zeta-potentials at pH = 9.3 and 7.4 were shown but far higher than those of M-MSNs. As pH was tuned to 4.2, M-MSNs-COOH showed positive charge. This result revealed that protonation of the residual amino groups took place in the acidic medium leading to the positively charged surface. In the case of the M-MSNs-PO_3^-, we observed the negative zeta-potentials were gradually decreasing with an increment of pH values. It was a consequence of the relatively low pK_a value (2.0) of -PO_3^- groups.[33] For M-MSNs-Ph, the zeta potentials were slightly reduced compared with M-MSNs at corresponding pH. The results indicated that there were still lots of residual silanol groups at the exterior surface of M-MSNs-Ph to afford the negative charge and colloidal stabilization. In line with the above discussion, we should highlight that the multiplex functional groups on the surface of modified M-MSNs underscore the key role to vary the charge densities and species. Thus, we anticipate that diversification of surface groups would bring the superior drug loading capacity and unique release behavior by virtue of the different drug-carriers interactions. This point would be discussed exhaustively below.

2. Drug loading and release experiments

2.1. DOX. Table 3 listed the DOX loading contents and entrapment efficiencies for three negatively charged samples. For M-MSNs, the loading content was 5.8% and the entrapment

Table 3 Results obtained from samples used for loading DOX

Sample	Loading content (%)	Entrapment efficiency (%)
M-MSNs	5.8	12.4
M-MSNs-COOH	10.5	23.6
M−MSNs−PO_3^-	31.0	89.8

efficiency was 12.4%. Interestingly, both parameters were remarkably increased to 10.5%, 23.6% for M-MSNs-COOH and 31.0%, 89.8% for M-MSNs-PO_3^-, respectively. This increasing tendency can be well explained by the electrostatic attraction between DOX and the modified M-MSNs. To our knowledge,[34] DOX has the pK_a of 8.3 and thus is positively charged at pH 7.4. As such, through the stronger electrostatic attraction, the loading contents were enhanced obviously for the modified M-MSNs. Indeed, the M-MSNs-PO_3^- displayed the extremely high entrapment efficiency (89.8%) as the feeding ratio of DOX and carriers was the same as another two cases. Also, there was higher pore volume to physically entrap more DOX molecules for M-MSNs-PO_3^- (1.03 $cm^3\ g^{-1}$) than that for M-MSNs-COOH (0.54 $cm^3\ g^{-1}$).

The pH-variable release profiles from DOX-loaded M-MSNs-COOH were shown in Fig. 3A. At pH = 9.3, the release amount was quite low and only approximately 3% was released in 120 h. Intriguingly note that when pH decreased from 7.4, 6.6 to 5.5, the drug release rates were increased and the release amounts arrived at 23.0%, 30.1% and 47.6% in 120 h, correspondingly. At pH 4.2, the sharp release in the initial stage was observed, and eventually the release amount reached as high as 56.7%. It is commonly known that DOX is dissolved in water at low pH, but insoluble in alkaline environment.[35] As a result, the insoluble DOX could not be freely distributed out of mesopores at pH = 9.3. On the other hand, another crucial point influenced the DOX release should be considered. As pH decreased to acidic range, the carboxyl group on the surface of M-MSNs-COOH was protonated so that the electrostatic attraction between the carriers and DOX was weakened. Thus, it was expected that the loaded DOX would be released at pH 4.2 freely, based on the lack of electrostatic attraction between the M-MSNs-COOH and DOX. In contrast, the DOX-loaded M-MSNs-PO_3^- showed different release behaviours (Fig. 3B). Due to the poor solubility of DOX at pH 9.3, the release amount was as low as 2.3%. As pH decreased to 7.4, 6.6, 5.5 and 4.2, all of release curves exhibited similar continued release behaviours in 120 h, and gave the release amounts as high as 45.2%, 51.2%, 54.9% and 57.1%, respectively. The relative rapid DOX release at pH = 7.4 was ascribed to the physical entrapment of DOX in the residual pore channels of M-MSNs-PO_3^-. The similar release behaviours in other acidic medium were attributed to the nearly unchanged electrostatic attraction between M-MSNs-PO_3^- and protonated DOX.

It is well known that the environment around tumours and other inflamed tissues in the body tends to be more acidic (pH = 5.5–6.5) relative to the normal physiological environment (pH = 7.4).[36] Therefore, we expect that the pH-sensitive release of drug-loaded M-MSNs-COOH opens up the opportunity in the tumour therapy.[37]

2.2. PTX. For M-MSNs, the loading content of PTX was 8.8% and the entrapment efficiency was 85.4%. The corresponding parameters were slightly decreased to 7.1% and 71.0% for M-MSNs-Ph. To the best of our knowledge, loading PTX within the M-MSNs could be induced by the interaction of hydrogen bonding between hydroxyl groups of PTX and silanol groups of M-MSNs.[38] Although there also presented certain extent of hydrophobic interaction between -Ph groups and PTX, the loading content of M-MSNs-Ph would be decreased correspondingly, when the silanol groups were reacted with PTS.

The release experiments of PTX loaded within M-MSNs and M-MSNs-Ph were conducted at 37 °C in PBS (pH = 7.4). In the inset of Fig. 4, the initial burst releases were observed in the first 1 h[39] and the release amount was 14.1% and 9.9% for the PTX-loaded M-MSNs and M-MSNs-Ph, respectively. In the following stage, when M-MSNs released less than 60% drug in 7 d, the M-MSNs-Ph had released mostly with nearly pH independent. It was well known that the initial burst release were ascribed to the adsorption of PTX on the external surface, while the subsequent slow release arised from the inner PTX resided in the mesopores. Thus, based on the strong hydrogen bonding interaction,[38] the

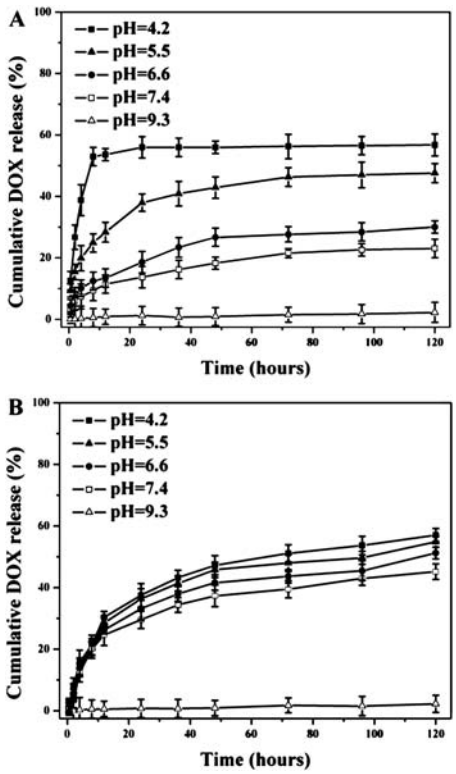

Fig. 3 pH-dependent cumulative DOX release from (A) M-MSNs-COOH and (B) M-MSNs-PO_3^-.

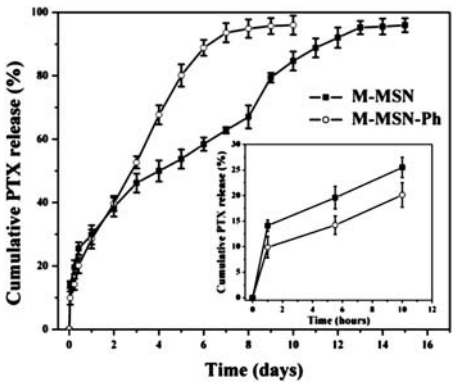

Fig. 4 PTX release from M-MSNs and M-MSNs-Ph. (inset: the PTX release in initial stage).

M-MSNs would load more PTX resulting in pronounced initial release content and quite slow release with time prolonging. In contrast, since the M-MSNs-Ph had a few of residual silanol groups, the poor affinity with PTX led to small release amount in the initial stage and high release rate afterwards. These results have an important implication that M-MSNs-Ph appears suited for a control over the sustained release of PTX for the tissue treatment in a short term than M-MSNs.

3. *In vitro* cell assay

The *in vitro* cellular cytotoxicity of the DOX-loaded M-MSNs-COOH and PTX-loaded M-MSNs-Ph to HeLa cells was investigated. The CCK-8 cell proliferation assay results (Fig. 5A) demonstrated that the M-MSNs-COOH carriers showed no cytotoxic effect on the HeLa cells even at 100 μg mL^{-1}. After 48 h incubations at a DOX dose of 0.1 μg mL^{-1}, the cell viability was 34% for DOX-loaded M-MSNs-COOH while less than the case of the pure DOX (3%). Also, IC_{50} value (the concentration of drugs required to reduce cell growth by 50%) for HeLa cells was determined to be 0.03 and 0.06 μg mL^{-1} for DOX and DOX-loaded M-MSNs-COOH, respectively. When combined with the release profiles of DOX-loaded M-MSNs-COOH (Fig. 3A), only 18% of DOX was released in 48 h at pH 7.4 and 43% of DOX at pH 5.5. Therefore, DOX-loaded M-MSNs-COOH displayed low cytotoxicity but enough efficiency to kill the cancer cells.

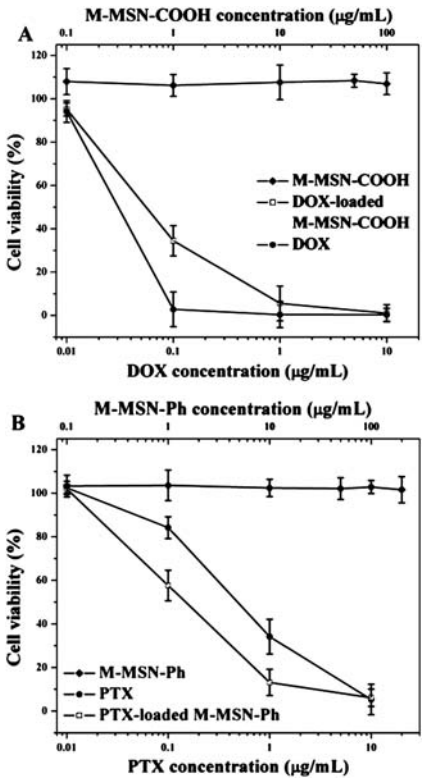

Fig. 5 HeLa cell survival assay. (A) (◆) M-MSNs-COOH in PBS, (●) free DOX in PBS, and (■) DOX-loaded M-MSNs-COOH in PBS. The concentration of M-MSNs-COOH was labelled at the top of the *x*-axis. (B) (◆) M-MSNs-Ph in PBS, (●) free PTX in PBS, and (■) PTX-loaded M-MSNs-Ph in PBS. The concentration of M-MSNs-Ph was labelled at the top of the *x*-axis.

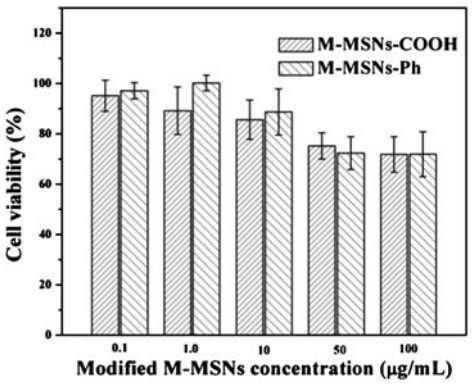

Fig. 6 Cell viability of HEK 293 cells exposed to M-MSNs-COOH and M-MSNs-Ph.

As shown in Fig. 5B, 13% of the HeLa cells were viable after 48 h exposure to 1 μg mL^{-1} PTX loaded in M-MSNs-Ph, whereas 34% of the cells remained viable when exposed to the same concentration of free PTX. IC_{50} values were 0.15 μg mL^{-1} for PTX-loaded M-MSNs-Ph and 0.48 μg mL^{-1} for free PTX. It was revealed that PTX-loaded M-MSNs-Ph exhibited the higher cytotoxic activity than free PTX. Considering the non-toxicity of M-MSNs-Ph to HeLa cells, we ascribed it to the hydrophobic character of PTX. The poor solubility in PBS lowered the drug concentration in cellular medium while the well dispersed PTX-loaded M-MSNs-Ph were quickly taken up by HeLa cells resulting in the intercellular sustained release of PTX. Lu group also reported the higher cytotoxic behaviour of the nanocarriers loading the hydrophobic anticancer drug than free drug.[11] As a result, the M-MSNs-Ph could maintain the pharmacological activity of PTX by endocytosing drug-loaded carriers to induce apoptosis. This superior performance undoubtedly enables M-MSNs-Ph as vehicles to store and deliver the water-insoluble anticancer drugs.

Furthermore, the cytotoxicity of M-MSNs-COOH and M-MSNs-Ph was also tested on normal HEK 293 cells. As shown in Fig. 6, the blank nanoparticles were almost non-toxic to HEK 293 cells at 0.1–10 μg mL^{-1}. As the concentration was 50 μg mL^{-1}, the cell viability was about 70%. These results demonstrated that the mesoporous nanoparticles were non-toxic materials at low concentrations, and on the other hand, slightly toxic at high concentrations.[40] It should be mentioned that the concentration of the mesoporous nanoparticles as drug platform to kill cancer cells effectively, was lower than 10 μg mL^{-1}, which was biocompatible to normal cells. The macrophage uptake of DOX-loaded M-MSNs-COOH by THP-1 cells was only 2% in 0.25 h, due to their high hydrophilicity,[41] and even after 4 h, the cell uptake was less than 2.5%. It can foresee that the mesoporous nanoparticles are long-circulating drug carriers for tumour therapy.

Conclusion

M-MSNs were synthesized through the sol–gel method and then functionalized with –COOH, $–PO_3^-$, $–NH_2$ and –Ph groups, respectively. The payload capacity and release behaviour of DOX and PTX as model drugs were found to be highly

dependent on the surface properties of mesoporous nanoparticles. For DOX, the electrostatic attraction for M-MSNs-COOH and M-MSNs-PO_3^- systems was beneficial for the drug loading, and also affected their release process. The unique pH-responsible release behaviour was apparently observed in the DOX-loaded M-MSNs-COOH system. For PTX, the hydrogen bonding interaction between PTX and silanol groups induced the variation in the payload capacity and the release behaviour. Compared with the relatively slow release in M-MSNs, M-MSNs-Ph, due to the weaker affinity with PTX, showed a quicker release rate in hydrophilic environment. The cytotoxicity of modified M-MSNs and macrophage uptake indicated that modified M-MSNs were suitable as drug carriers. When compared with the control set of experiments with equivalent doses of drugs, DOX-loaded M-MSNs-COOH had the lower cell toxicity to HeLa cells, while PTX-loaded M-MSNs-Ph allowed the higher one. This implied that the modified M-MSNs satisfied the different requirement on the release of hydrophilic and hydrophobic drugs, *i.e.* a sustained release and improved release rate in physiological medium, respectively. Therefore, these mesoporous nanoparticles were suitable to store hydrophilic and hydrophobic anticancer drugs for drug delivery and cancer treatment.

Acknowledgements

We are grateful for the support of the National Science Foundation of China (grant no. 50403011, 20874015), the Shanghai Rising-Star Program (10QH1400200), the Innovation Program of Shanghai Municipal Education Commission (09ZZ01).

References

1 J. Kim, Y. Piao and T. Hyeon, *Chem. Soc. Rev.*, 2009, **38**, 372–390.
2 H. Maeda, J. Wu, T. Sawa, Y. Matsumura and K. Hori, *J. Controlled Release*, 2000, **65**, 271–284.
3 R. Duncan, *Nat. Rev. Drug Discovery*, 2003, **2**, 347–360.
4 A. K. Patri, J. F. Kukowska-Latallo and J. R. Baker, *Adv. Drug Delivery Rev.*, 2005, **57**, 2203–2214.
5 V. P. Torchilin, *Nat. Rev. Drug Discovery*, 2005, **4**, 145–160.
6 J. Salonen, L. Laitinen, A. M. Kaukonen, J. Tuura, M. Bjorkqvist, T. Heikkila, K. Vaha-Heikkila, J. Hirvonen and V. P. Lehto, *J. Control. Release*, 2005, **108**, 362–374.
7 L. Bromberg, M. Temchenko and T. A. Hatton, *Langmuir*, 2002, **18**, 4944–4952.
8 I. I. Slowing, J. L. Vivero-Escoto, C. W. Wu and V. S. Y. Lin, *Adv. Drug Delivery Rev.*, 2008, **60**, 1278–1288.
9 K. S. Finnie, D. J. Waller, F. L. Perret, A. M. Krause-Heuer, H. Q. Lin, J. V. Hanna and C. J. Barbe, *J. Sol-Gel Sci. Technol.*, 2009, **49**, 12–18.
10 M. Vallet-Regi, F. Balas and D. Arcos, *Angew. Chem., Int. Ed.*, 2007, **46**, 7548–7558.
11 J. Lu, M. Liong, J. I. Zink and F. Tamanoi, *Small*, 2007, **3**, 1341–1346.
12 M. Liong, S. Angelos, E. Choi, K. Patel, J. F. Stoddart and J. I. Zink, *J. Mater. Chem.*, 2009, **19**, 6251–6257.
13 S. Huh, J. W. Wiench, J. C. Yoo, M. Pruski and V. S. Y. Lin, *Chem. Mater.*, 2003, **15**, 4247–4256.
14 J. Kecht, A. Schlossbauer and T. Bein, *Chem. Mater.*, 2008, **20**, 7207–7214.
15 J. C. Doadrio, E. M. B. Sousa, I. Izquierdo-Barba, A. L. Doadrio, J. Perez-Pariente and M. Vallet-Regi, *J. Mater. Chem.*, 2006, **16**, 462–466.
16 P. Horcajada, A. Ramila, F. Gerard and M. Vallet-Regi, *Solid State Sci.*, 2006, **8**, 1243–1249.
17 F. Hoffmann, M. Cornelius, J. Morell and M. Froba, *Angew. Chem., Int. Ed.*, 2006, **45**, 3216–3251.
18 B. Munoz, A. Ramila, J. Perez-Pariente, I. Diaz and M. Vallet-Regi, *Chem. Mater.*, 2003, **15**, 500–503.
19 S. Mornet, S. Vasseur, F. Grasset and E. Duguet, *J. Mater. Chem.*, 2004, **14**, 2161–2175.
20 Z. Li, L. Wei, M. Y. Gao and H. Lei, *Adv. Mater.*, 2005, **17**, 1001–1005.
21 A. H. Lu, W. Schmidt, N. Matoussevitch, H. Bonnemann, B. Spliethoff, B. Tesche, E. Bill, W. Kiefer and F. Schuth, *Angew. Chem., Int. Ed.*, 2004, **43**, 4303–4306.
22 S. Bucak, D. A. Jones, P. E. Laibinis and T. A. Hatton, *Biotechnol. Prog.*, 2003, **19**, 477–484.
23 J. Kim, J. E. Lee, S. H. Lee, J. H. Yu, J. H. Lee, T. G. Park and T. Hyeon, *Adv. Mater.*, 2008, **20**, 478–483.
24 J. Kim, J. E. Lee, J. Lee, J. H. Yu, B. C. Kim, K. An, Y. Hwang, C. H. Shin, J. G. Park, J. Kim and T. Hyeon, *J. Am. Chem. Soc.*, 2006, **128**, 688–689.
25 M. Liong, J. Lu, M. Kovochich, T. Xia, S. G. Ruehm, A. E. Nel, F. Tamanoi and J. I. Zink, *ACS Nano*, 2008, **2**, 889–896.
26 S. B. Wang, *Microporous Mesoporous Mater.*, 2009, **117**, 1–9.
27 W. M. Zheng, F. Gao and H. C. Gu, *J. Magn. Magn. Mater.*, 2005, **288**, 403–410.
28 C. Y. Liu, J. Guo, W. L. Yang, J. H. Hu, C. C. Wang and S. K. Fu, *J. Mater. Chem.*, 2009, **19**, 4764–4770.
29 N. Lang and A. Tuel, *Chem. Mater.*, 2004, **16**, 1961–1966.
30 J. Kobler, K. Moller and T. Bein, *ACS Nano*, 2008, **2**, 791–799.
31 J. M. Rosenholm and M. Linden, *J. Controlled Release*, 2008, **128**, 157–164.
32 K. K. Sharma and T. Asefa, *Angew. Chem., Int. Ed.*, 2007, **46**, 2879–2882.
33 R. P. Bagwe, L. R. Hilliard and W. H. Tan, *Langmuir*, 2006, **22**, 4357–4362.
34 A. Choucair, P. L. Soo and A. Eisenberg, *Langmuir*, 2005, **21**, 9308–9313.
35 L. B. Chen, F. Zhang and C. C. Wang, *Small*, 2009, **5**, 621–628.
36 S. Ganta, H. Devalapally, A. Shahiwala and M. Amiji, *J. Controlled Release*, 2008, **126**, 187–204.
37 S. M. Simon, *Drug Discovery Today*, 1999, **4**, 32–38.
38 H. Hata, S. Saeki, T. Kimura, Y. Sugahara and K. Kuroda, *Chem. Mater.*, 1999, **11**, 1110–1119.
39 F. Danhier, N. Lecouturier, B. Vroman, C. Jerome, J. Marchand-Brynaert, O. Feron and V. Preat, *J. Controlled Release*, 2009, **133**, 11–17.
40 S. P. Hudson, R. F. Padera, R. Langer and D. S. Kohane, *Biomaterials*, 2008, **29**, 4045–4055.
41 M. Shi, J. Lu and M. S. Shoichet, *J. Mater. Chem.*, 2009, **19**, 5485–5498.